Environment and Natural Resources Journal

Volume 23
Issue 1
2025

# Analyzing Drought Propagation and Its Influential Factors in the Upper Nan Watershed, Thailand

**Muhammad Chrisna Satriagasa, Piyapong Tongdeenok*, and Naruemol Kaewjampa**

*Watershed and Environmental Management Program, Faculty of Forestry, Kasetsart University, Bangkok 10900, Thailand*

**ARTICLE INFO**

Received: 15 Jul 2024
Received in revised: 4 Oct 2024
Accepted: 16 Oct 2024
Published online: 11 Dec 2024
DOI: 10.32526/ennrj/23/20240202

**Keywords:**
Meteorological drought/ Hydrological drought/ Drought propagation/ Upper Nan Watershed/ Forest conservation

*** Corresponding author:**
E-mail: fforppt@ku.ac.th

**ABSTRACT**

Understanding drought propagation is essential for effective water resource management. This study employs an innovative approach to examine the transition from meteorological drought (MD) to hydrological drought (HD) in the Upper Nan Watershed (UNW), Thailand, using the standardized precipitation evapotranspiration index (SPEI) and standardized streamflow index (SSI). Cross-wavelet transform (XWT) and Pearson's correlation analyses reveal a significant positive correlation between MD and HD, with the drought propagation time (DPT) ranging from 2 to 5 months, notably shorter during the dry season. The eastern UNW (Zone I) has the longest DPT, while the western UNW (Zone III) has the shortest. This study is distinguished by its integration of global teleconnection factors, such as El Niño-Southern Oscillation (ENSO), the Dipole Mode Index (DMI), and Pacific Decadal Oscillation (PDO), alongside local factors like climate, slope, and watershed morphometry. This dual focus provides a comprehensive analysis of drought dynamics, enhancing the understanding of drought propagation and its complexities. The integration of global and local influences provides insights applicable across diverse water resource management contexts. It highlights the critical role of forests in regulating water flow and extending the DPT, emphasizing the need for forest conservation and land use regulation in the headwaters. Despite challenges associated with highland meteorological data, findings offer improvements to existing drought monitoring and early warning systems, underscoring the importance of combining global and local factors in effective drought management strategies.

## 1. INTRODUCTION

Drought, characterized by insufficient rainfall, leads to significant water shortages that affect agriculture, the environment, and society and result in substantial economic losses (Dalezios et al., 2012). The types of drought include meteorological drought (MD), agricultural drought, hydrological drought (HD), and socioeconomic drought, occurring when water supply fails to meet demand (Abbas and Kousar, 2021). Understanding the transition from MD to HD is critical for water resource management. However, previous studies have not explored the combination of global and local factors affecting drought propagation, especially in the context of Thailand's Upper Nan Watershed (UNW). This study bridges that gap by offering an innovative and detailed analysis of the dynamics between global teleconnection factors and local watershed conditions to predict drought propagation.

Previous studies have explored drought propagation, with Ding et al. (2021a) finding stronger propagation from agricultural drought (AD) to HD in northern China during summer and autumn; Huang et al. (2017) noting a time lag between MD and HD in the Wei River Basin, influenced by atmospheric anomalies such as El Niño-Southern Oscillation (ENSO) and Arctic Oscillation (AO); and Gu et al. (2020) showing that droughts increase in duration and severity as they propagate, particularly in the Yangtze and Yellow River basins. This research contributes to

**Citation:** Satriagasa MC, Tongdeenok P, Kaewjampa N. Analyzing drought propagation and its influential factors in the Upper Nan Watershed, Thailand. Environ. Nat. Resour. J. 2025;23(1):14-27. (https://doi.org/10.32526/ennrj/23/20240202)

the field by focusing on the UNW, a drought-prone area in Thailand where the specific dynamics of MD-to-HD propagation are not yet well understood. Climate change intensifies droughts, affecting water availability and agricultural productivity (Wan et al., 2018; Xu et al., 2019). Land use changes such as deforestation and urbanization worsen drought impacts by disrupting hydrological cycles and reducing water retention (Fedele et al., 2018).

The UNW in northern Thailand flows from north to south, merging with the Wang, Ping, and Yom Watersheds to form the Chao Phraya Watershed. This study presents an innovative approach by examining the spatiotemporal mechanisms of drought propagation in the UNW and identifying the factors affecting the drought propagation time (DPT). This novel combination of global factors (e.g., ENSO, DMI, and PDO) with local conditions such as topography and land use provides a fresh perspective on drought management. Using the SPEI, the SSI, cross-wavelet transform (XWT), and Pearson's correlation analyses, this research aims to improve drought monitoring and early warning systems. The findings will inform land use policies and forest conservation to reduce the socio-economic impacts of drought in the UNW and similar watersheds, delivering insights for enhancing integrated drought management strategies globally.

## 2. METHODOLOGY

### 2.1 Study area

This study was conducted in the Upper Nan Watershed (UNW) in northern Thailand; it spans the coordinates 18°27′55.72″ N to 19°38′26.97″ N and 100°21′39.14″ E to 101°21′7.52″ E, covering an area of 4,588.4 km² (Figure 1). The UNW experiences a dry season (January to March and November to December) with 9.7 to 64.4 mm of rainfall and a wet season (April to October) with 102.7 to 269 mm, often receiving rainstorms from the South China Sea during the northeast monsoon. The landscape includes hilly upstream and midstream regions and low-lying flatland downstream, where the town of Nan is located. The headwaters are critical due to the thin soil from intensive erosion on steep slopes, which limits moisture retention and increases drought susceptibility. Agriculture is vital in the UNW, with rice and maize being the primary crops. Forests have been cleared for maize cultivation due to its higher economic returns, leading to reduced soil moisture retention, increased runoff, and soil erosion, heightening drought vulnerability (Paiboonvorachat and Oyana, 2011). The region heavily relies on agriculture, stressing water resources and necessitating sustainable management for long-term environmental and economic stability (Plangoen and Babel, 2014; Satriagasa et al., 2023).

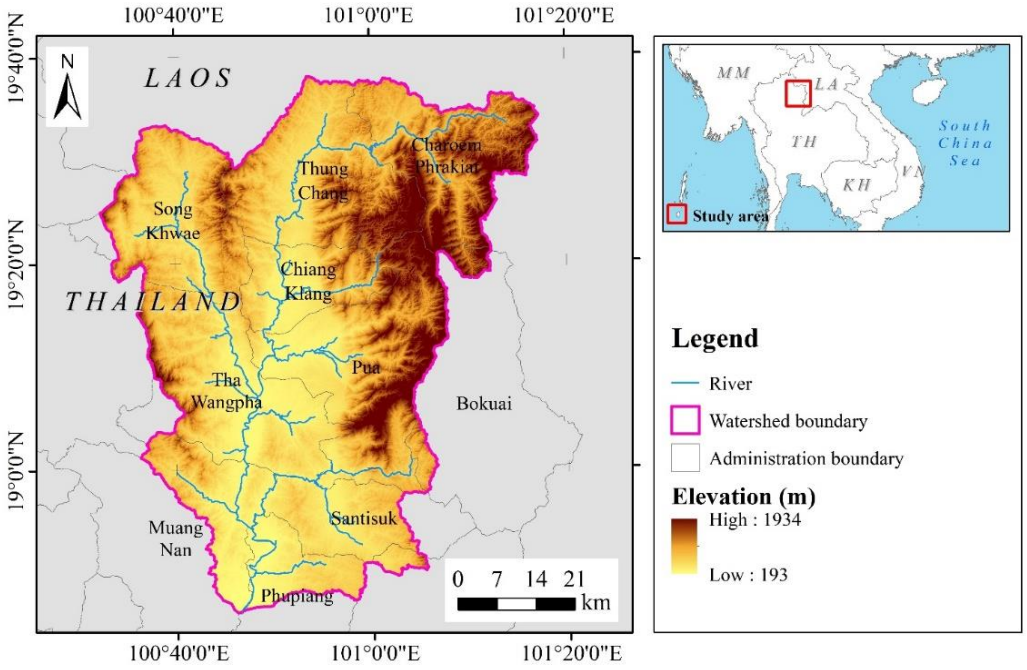


**Figure 1.** Map of Upper Nan Watershed

## 2.2 Data collection

Several types of data were used in this study, detailed in Table 1.

The data used in this study span the period from 2000 to 2020, covering 21 years. While a 30-year or longer time series is generally recommended for calculating drought indices to better assess long-term trends, the selection of this period was driven by several key considerations.

First, data availability was a significant factor. Reliable and continuous meteorological and hydrological data, particularly for highland areas within the Upper Nan Watershed, only became consistently available in 2000. Prior to this, there were substantial gaps in the dataset, which could have introduced uncertainty and reduced the accuracy of the drought index calculations.

Second, the selected period provides consistent and continuous datasets for both meteorological and hydrological parameters, ensuring the reliability of the cross-wavelet transform (XWT) and Pearson's correlation analyses performed in this study. Extending the dataset beyond 2000 would require incorporating older, inconsistent data that could negatively affect the robustness of the results.

**Table 1.** Data used in this study, period, and data source

| No | Data | Period | Source |
|---|---|---|---|
| 1 | Rainfall data from CHIRPS imagery | 2000-2020 | Climate Hazard Center UC Santa Barbara (https://chc.ucsb.edu/data/chirps) |
| 2 | Air temperature data from ERA5 imagery | 2000-2020 | Copernicus (https://cds.climate.copernicus.eu/), acquired in Google Earth Engine |
| 3 | Sea surface temperature (SST) data | 2000-2020 | Physical Science Laboratory of the NOAA (https://psl.noaa.gov/gcos_wgsp/Timeseries/) |
| 4 | Dipole mode index (DMI) data | 2000-2020 | |
| 5 | Pacific decadal oscillation (PDO) data | 2000-2020 | National Center for Environmental Information of the NOAA(https://www.ncei.noaa.gov/access/monitoring/pdo/) |
| 6 | Streamflow data | 2000-2020 | Observed streamflow data from Thailand Royal Irrigation Department (RID) (https://www.hydro-1.net/), SWAT-modeled streamflow from (Satriagasa et al., 2023) |
| 7 | Hansen Global Forest Change | 2000-2020 | Hansen et al. (2013) |
| 8 | DEM SRTM 30 m | - | USGS (https://www.usgs.gov/) |

Finally, this period captures recent climate trends, particularly the increasing frequency and intensity of drought events influenced by global teleconnection factors such as ENSO, the DMI, and PDO. Focusing on the period from 2000 to 2020 allows for a more relevant assessment of recent drought propagation dynamics and provides insights that are applicable to current and future drought management strategies.

For rainfall data, this study used CHIRPS satellite-based precipitation estimates from the Climate Hazard Center at UC Santa Barbara. While CHIRPS provides extensive spatial and temporal coverage, we did not conduct a formal validation process comparing CHIRPS data to local measurements. However, CHIRPS has been widely used and validated in similar regions, including Southeast Asia, for its ability to represent precipitation patterns and drought conditions. Although satellite-based estimates have limitations, they offer significant advantages in areas such as the Upper Nan Watershed, where ground-based meteorological stations are sparse.

In choosing CHIRPS data, we balanced data consistency and availability with the need to capture relevant drought events and climatic trends during the study period. Future studies could enhance these findings by conducting additional validations with local rainfall measurements.

While a longer time series would be ideal for long-term trend analysis, the 21-year period used in this study represents a balance among data quality, consistency, and relevance to the changing climatic conditions in the region.

## 2.3 Drought indices

### *2.3.1 Standardized precipitation evapo-transpiration index (SPEI)*

The standardized precipitation evapo-transpiration index (SPEI) is widely used for detecting meteorological drought (MD). As proposed by Vicente-Serrano et al. (2010), it incorporates temperature-induced evapotranspiration with rainfall,

enhancing drought detection accuracy. The SPEI calculation involves computing the difference between precipitation (P) and potential evapotranspiration (PET) for each month (Equation 1), aggregating these values over different timescales (1 to 12 months), fitting the accumulated values to a log-logistic probability distribution (Equation 2), and converting them into a standardized index with a mean of zero and a standard deviation of one (Equation 3). This study used the SPEI to assess MD in the UNW from 2000 to 2020 over 1- to 12-month periods, with calculations performed using the SPEI package in RStudio for rapid, accurate, and reliable results.

$$D = P - PET \quad (1)$$

$$F(x) = \frac{1}{1+\left(\frac{\alpha}{x-\gamma}\right)^{\beta}} \quad (2)$$

$$SPEI = \frac{W-\mu}{\sigma} \quad (3)$$

Where; F(x) is the cumulative probability, x is the water balance, and α, β, and γ are the scale, shape, and location parameters, respectively; W is the log-logistically normalized water balance, μ is the mean, and σ is the standard deviation.

*2.3.2 Standardized streamflow index (SSI)*

The standardized streamflow index (SSI) captures hydrological drought (HD) by analyzing streamflow discharge. On the basis of monthly streamflow data modeled using the soil and water assessment tool (SWAT) for the period from 2000 to 2020, the SSI was calculated for the Upper Nan Watershed (UNW) following the standardized precipitation index (SPI) method. The steps include collecting monthly streamflow data, aggregating it over the chosen timescale, normalizing it to a probability distribution (typically log-normal), and standardizing it to a mean of zero and standard deviation of one, resulting in SSI values (Equation 4).

$$SSI = \frac{Q-\mu}{\sigma} \quad (4)$$

Where; Q is the monthly streamflow value, μ is the mean of the streamflow over the reference period, and σ is the standard deviation of the streamflow.

The SWAT model was run with a warm-up period from 1980 to 1984 to initialize the model. Calibration was conducted for 1985 to 2005 and validation for 2006 to 2020 using observed streamflow data from the Thailand Royal Irrigation Department (RID). The model's performance was assessed using the Nash-Sutcliffe Efficiency (NSE), the ratio of the root-mean-square error to the standard deviation (RSR), and the Kling-Gupta Efficiency (KGE). The calibration results showed an NSE of 0.83 (very good), an RSR of 0.59 (good), and a KGE of 0.45 (poor). For the validation period, the model achieved an NSE of 0.87 (very good), an RSR of 0.5 (very good), and a KGE of 0.53 (intermediate). These results confirmed that the SWAT model performed well in simulating streamflow during both the calibration and validation periods, providing confidence in its reliability for drought analysis in the UNW.

One month of SSI data was focused on to detect the propagation time from meteorological drought (MD) to HD using the SPEI/SPI package in RStudio. The SSI's reliability in hydrological drought assessment has previously been validated in various regions (Kartika and Wijayanti, 2023).

**2.4 Drought propagation time**

The drought propagation time (DPT) was determined using the maximum Pearson's correlation coefficient (MPCC) method. The SPEI was used to represent MD, and the SSI was used to represent HD. The MPCC—the highest Pearson correlation coefficient between the SPEI and SSI—then indicated the specific month of drought propagation. The MPCC values were calculated for 176 grid cells (each cell being 5.5 × 5.5 km) to determine the spatial distribution. Seasonal variations were captured by computing MPCC values for the entire year, dry season, and wet season.

The spatial distribution of the DPT in the study area showed notable variation across different parts of the watershed. To capture these variations more effectively, the area was divided into four distinct regions based on a combination of parameters. These parameters included the spatial distribution of the DPT itself, as well as other key environmental factors such as slope and topography, land use patterns, and forest cover. Regions with steeper slopes tended to have faster runoff and shorter DPTs, while flatter areas exhibited longer DPTs. Similarly, differences in land use—particularly between agricultural and forested areas—played a role in shaping water retention and flow dynamics, with areas of higher forest cover typically experiencing longer DPTs due to their better water retention capabilities. Areas with significant deforestation, in contrast, showed quicker drought

propagation. By combining these factors, each of the four regions reflects a distinct set of environmental conditions that influence drought behavior. This classification also provides a foundation for more targeted, region-specific drought mitigation strategies.

### 2.5 Drought propagation relationship

The relationship between meteorological drought (MD) and hydrological drought (HD) was analyzed using cross-wavelet transform (XWT) on data from 25 sub-watersheds in the UNW with RStudio. XWT identifies phase relationships between the standardized precipitation evapotranspiration index (SPEI) and the standardized streamflow index (SSI), showing drought propagation over time. The analysis assumed stationarity in the time series data and significant wavelet coherence. Figure 2 details the XWT procedure for characterizing drought propagation.

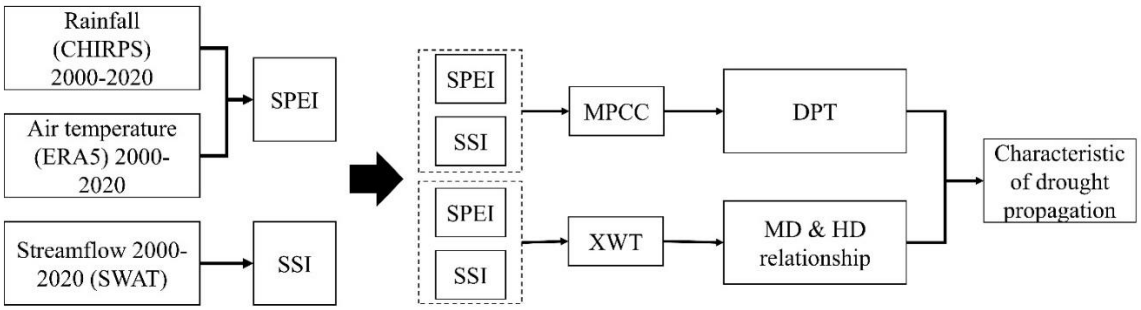


**Figure 2.** Procedure for characterizing drought propagation

### 2.6 Factor influencing drought propagation

Several factors influencing drought propagation were analyzed, including climatic, ecological, physical, and anthropogenic factors. The selection of El Niño-Southern Oscillation (ENSO), the Dipole Mode Index (DMI), and Pacific Decadal Oscillation (PDO) as teleconnection indices was based on their well-established influence on precipitation and temperature patterns in Southeast Asia, including Thailand. These indices were obtained from publicly available datasets, with ENSO data sourced from the National Oceanic and Atmospheric Administration (NOAA), DMI from the Physical Science Laboratory of NOAA, and PDO from the National Centers for Environmental Information (NCEI). The analysis involved correlating these teleconnection indices with local climate data by using cross-wavelet transform (XWT) to examine how variations in the teleconnection factors influenced drought propagation patterns over time. This approach allowed us to identify phase relationships and time lags between global teleconnection factors and local drought conditions.

Ecological and anthropogenic factors, such as forest cover, forest loss, and land use, were examined using data from Hansen Global Forest Change (Hansen et al., 2013) and Google Earth Engine. Forest cover change and deforestation rates were spatially analyzed to assess their influence on water retention and drought propagation. This was performed by overlaying forest cover maps onto drought propagation data and identifying regions where forest loss accelerated drought conditions. Anthropogenic activities, including land use changes for agriculture, were assessed using land use classifications provided by national databases and satellite imagery, with a focus on how these changes disrupted hydrological cycles.

Physical factors, including slope and watershed morphometry, were analyzed using high-resolution digital elevation models (DEMs) from the United States Geological Survey (USGS). A slope analysis was performed using ArcGIS to quantify how the topography influenced runoff and water retention in different sub-watersheds. The watershed morphometry was calculated using standard hydrological metrics, such as the drainage density, elongation ratio, and relief ratio, to evaluate how the physical structure of the watershed affected the speed and extent of drought propagation. These analyses provided a comprehensive understanding of drought propagation mechanisms in the UNW, integrating spatial and temporal assessments to determine their impacts.

## 3. RESULTS AND DISCUSSION

### 3.1 Result

*3.1.1 Drought propagation time (DPT)*

The drought propagation time (DPT) is the duration of the transition from meteorological drought (MD) to hydrological drought (HD). In this study, the

DPT was assessed in monthly steps from 1 to 12 months. Based on the maximum Pearson's correlation coefficient (MPCC) analysis, the DPT in the Upper Nan Watershed (UNW) ranges from 2 to 11 months (Figure 3(a)). The most common DPT is 2 to 5 months, with a 2-month DPT covering nearly 46% of the UNW, primarily in the middle part of the watershed. Upstream areas show greater variability, with four months dominating the west and three months dominating the east. Downstream, the DPT extends to five months. The MPCC values ranged from 0.35 to 0.64, indicating the strength of the relationship between the standardized precipitation evapotranspiration index (SPEI) and the standardized streamflow index (SSI). The highest MPCC values were found in the western upstream and midstream areas, while the rest of the watershed had low to medium values (Figure 4).

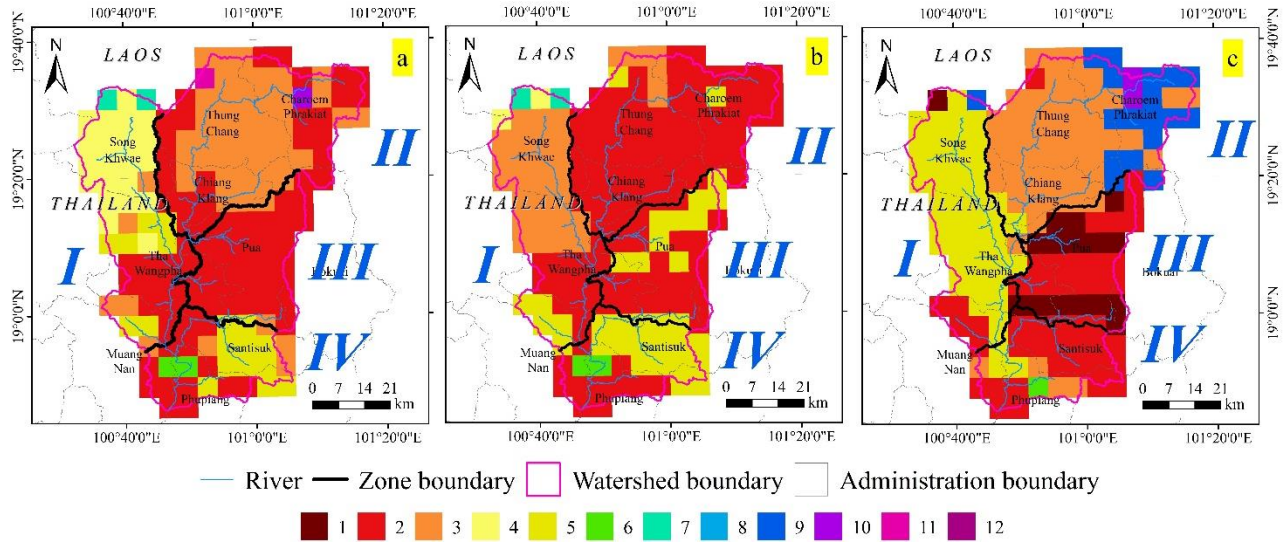


**Figure 3.** Spatial distribution of drought propagation time in month: (a) all seasons, (b) dry season, and (c) wet season

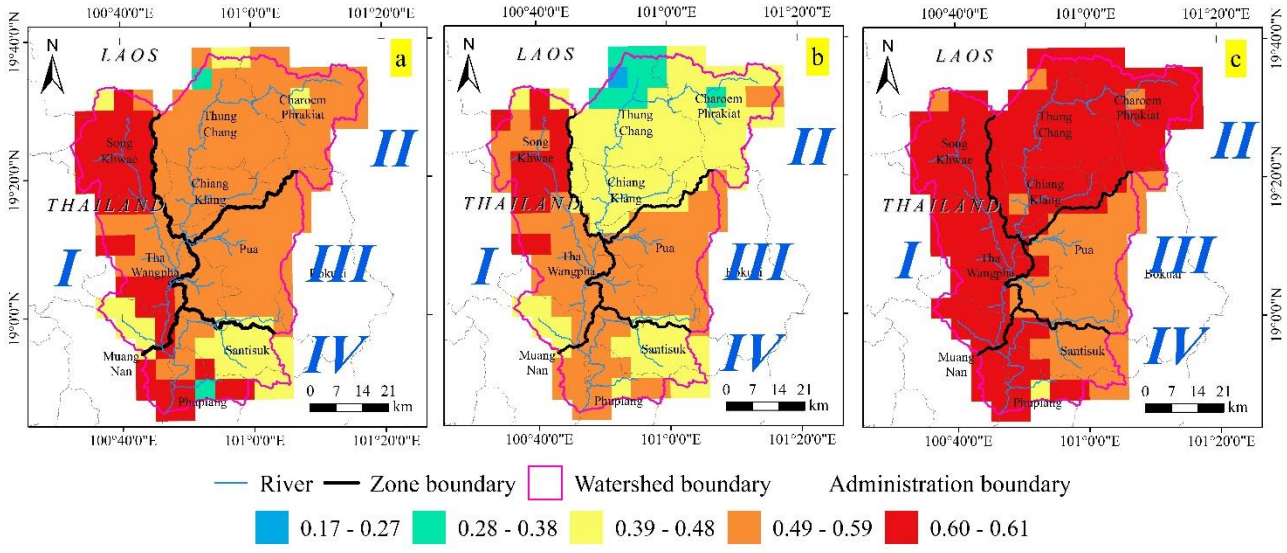


**Figure 4.** Spatial distribution of MPCC between SPEI and SSI: (a) all seasons, (b) dry season, and (c) wet season

*3.1.2 Seasonal drought propagation time*

To understand seasonal variations in the DPT, the standardized precipitation evapotranspiration index (SPEI) and standardized streamflow index (SSI) were analyzed for the dry (October-March) and wet (April-September) seasons. In the dry season, the DPT ranges from 2 to 7 months, with a 2-month DPT covering 60% of the watershed, indicating quicker drought propagation due to lower rainfall and higher temperatures. In the wet season, the DPT ranges from

1 to 10 months, with a 3-month DPT covering 30% of the watershed, suggesting that increased rainfall and soil moisture delay hydrological drought. The spatial distribution of the DPT reveals four distinct zones within the UNW, with MPCC values ranging from 0.17 to 0.61 in the dry season and 0.39 to 0.69 in the wet season, being highest in the western watershed. These patterns highlight the varying influences of precipitation, temperature, streamflow, and soil moisture on drought propagation.

*3.1.3 Meteorological and hydrological drought relationship*

A cross-wavelet transform (XWT) analysis of 25 SPEI and SSI dataset pairs revealed a positive correlation between MD and HD. Four representative XWT charts for the different zones show this correlation, with phase arrows predominantly pointing to the right (Figure 5). For full cross-wavelet transforms between SPEI and SSI, please refer to Figure S1 in the appendix section.

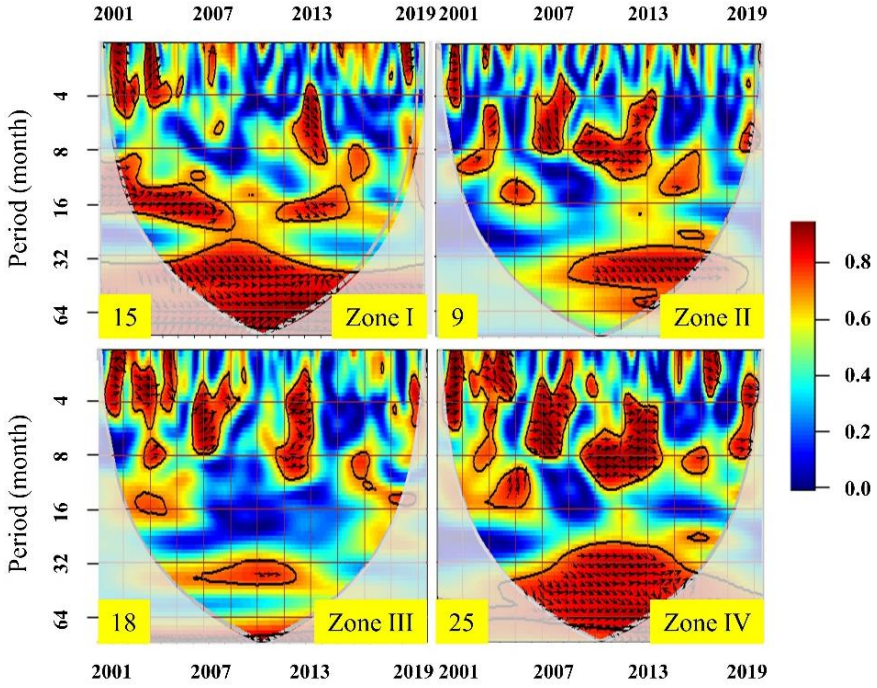


**Figure 5.** The cross-wavelet transforms between SPEI and SSI of zones I to IV. The arrows indicate the relative phase relationship, with right-pointing arrows representing positive correlations.

*3.1.4 Factor influencing the drought propagation characteristics*

Several factors influence drought propagation in the UNW, including climatic, ecological, physical, and anthropogenic factors. Our analysis primarily focused on the spatial relationships between these factors and drought propagation, using tools such as XWT and spatial overlays, rather than conducting a detailed quantitative analysis to ascertain the specific contribution of each factor. While statistical modeling could provide more precise measurements of each factor's impact, the current study aimed to identify and visualize spatial patterns that influence drought propagation.

Climatic factors, such as rainfall and air temperature, and global teleconnection indices, such as El Niño-Southern Oscillation (ENSO), the Indian Ocean Dipole (IOD), and Pacific Decadal Oscillation (PDO), significantly impact the region's water balance. El Niño phases reduce rainfall and raise temperatures, exacerbating drought conditions, while La Niña phases increase rainfall, mitigating drought. Similarly, positive IOD phases and warm PDO phases reduce precipitation and increase temperatures, worsening drought, while negative IOD and cool PDO phases alleviate drought. The temporal (Figure 6(a)) and spatial (Figure 7) rainfall patterns illustrate how these teleconnection factors affect the UNW's water balance by influencing the timing and severity of drought propagation.

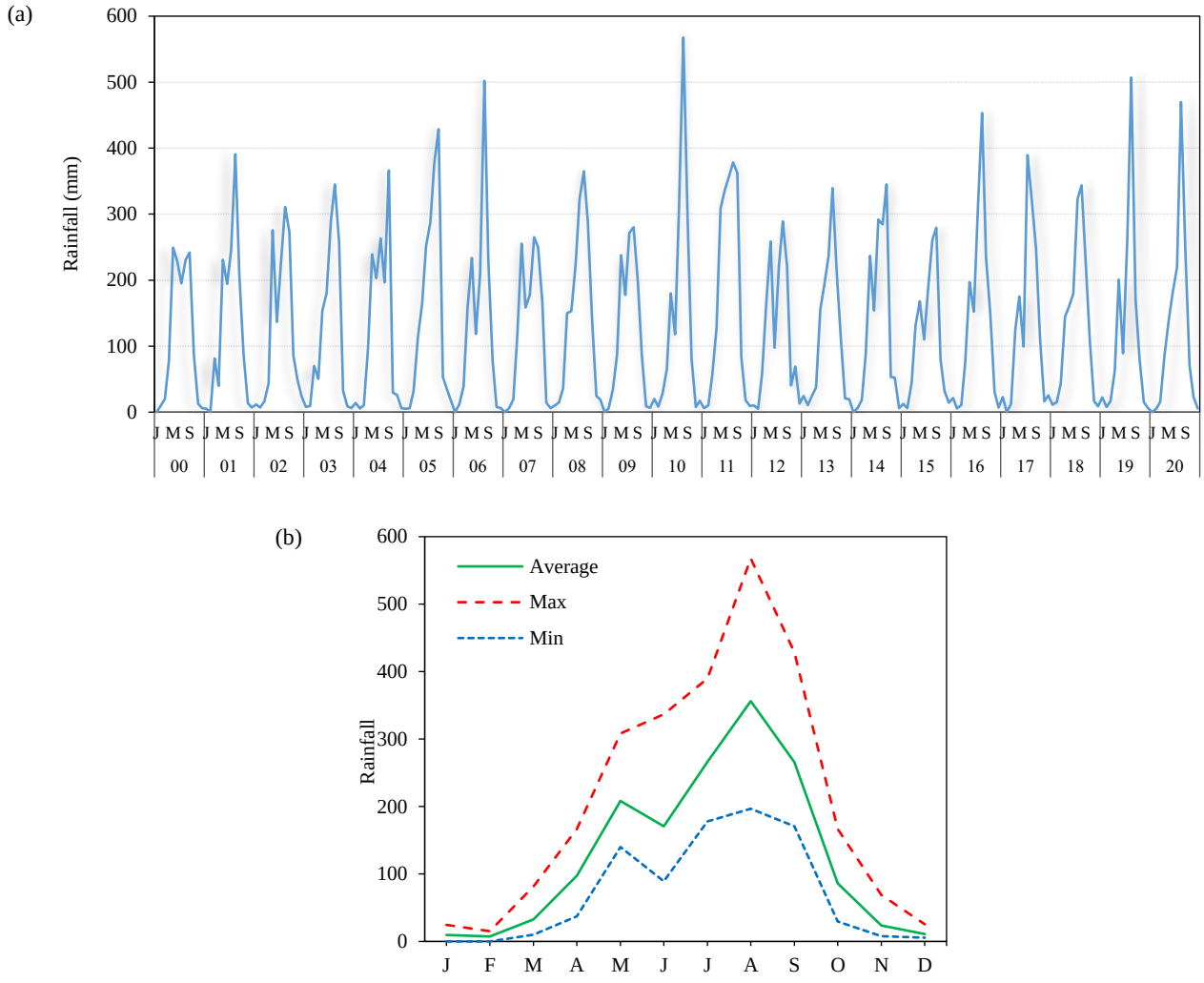


**Figure 6.** Temporal rainfall pattern of UNW: (a) annual and (b) monthly

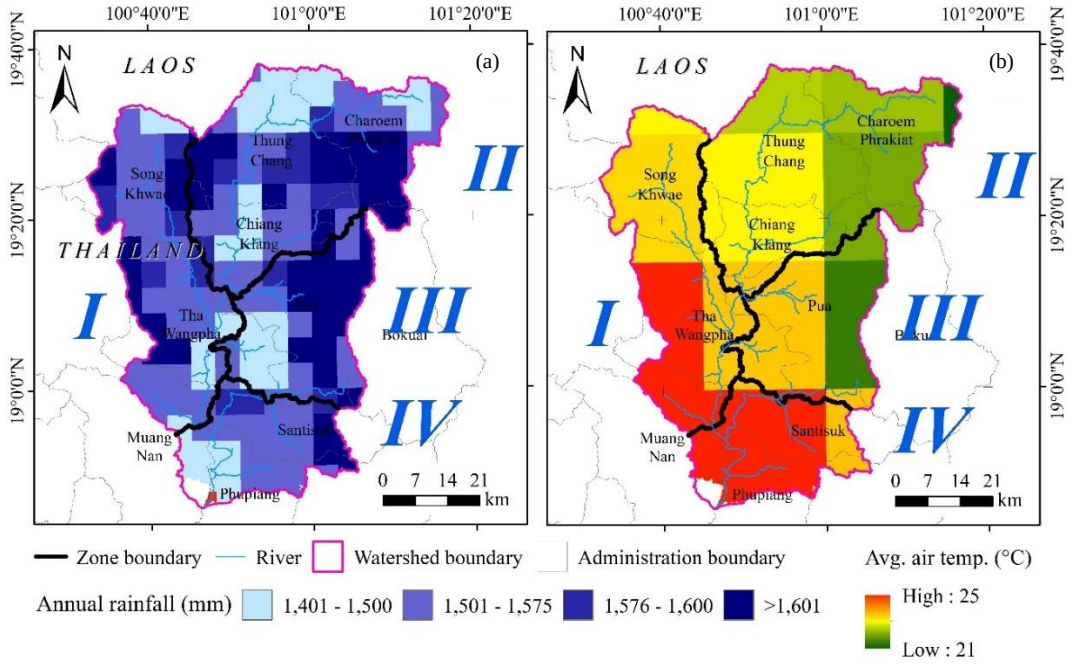


**Figure 7.** Spatial distribution of (a) annual rainfall and (b) average annual air temperature in the UNW

The annual rainfall in the UNW varies, with mountainous areas receiving over 1,600 mm and lowland areas near the outlet receiving 1,400-1,500 mm. The average temperatures range from 21°C upstream to 25°C downstream. Teleconnection factors such as ENSO, the DMI, and PDO exacerbate drought conditions. Understanding these factors is crucial for effective water management and climate adaptation. The XWT analysis showed significant negative correlations between all teleconnection factors, rainfall, and evaporation in the UNW (Figure 8).

Ecological factors, such as forest cover and forest loss, also play a critical role in regulating water retention and drought propagation. As shown in Figure 9(a), Zones I, II, and III have high tree cover with low forest loss, which helps delay drought propagation, while Zone IV, with extensive forest loss and dryland farming, experiences faster drought propagation. Although our analysis effectively highlights these spatial patterns, further quantitative analyses of the specific contributions of these factors could be explored in future studies.

The slope and watershed morphometry affect the DPT, with gentler slopes retaining water for longer and steep slopes causing rapid runoff (Figure 9(b)). Table 2 provides the detailed morphometric characteristics of selected sub-watersheds within the UNW, highlighting key metrics such as the maximum stream order (MSO), drainage density (DD), circulatory ratio (CR), elongation ratio (ER), and relief ratio (RR). These metrics help to explain why certain sub-watersheds, such as SW13, are highly prone to drought: their high relief ratio and low drainage density accelerate runoff and reduce water retention. For full Upper Nan Watershed morphometry, please refer to Table S1 in the appendix section.

In contrast, sub-watersheds such as SW15 and SW25 have gentler slopes, lower relief ratios, and better water retention capabilities, making them less prone to HD. Understanding these morphometric differences are crucial in determining how the physical characteristics of the watershed influence drought vulnerability and propagation, as reflected in the DPT across the various sub-watersheds. These physical characteristics were analyzed using DEMs and other spatial analysis techniques. While the spatial analysis effectively highlighted these relationships, a more detailed quantitative analysis of the specific contributions of each factor could be explored in future studies to provide a clearer understanding of the factors' impacts on drought propagation.

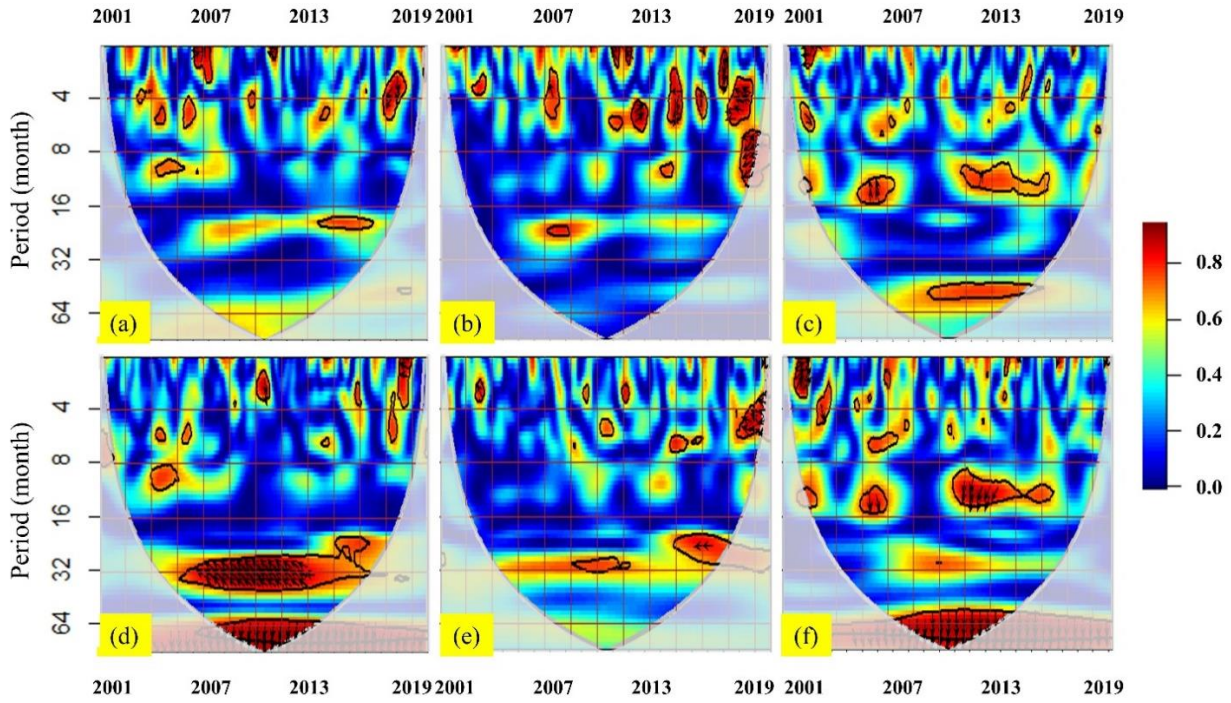


**Figure 8.** The cross wavelet transforms between (a) ATE and ENSO, (b) ATE and DMI, (c) ATE and PDO (d) rainfall and ENSO, (e) rainfall and DMI, and (f) rainfall and PDO.

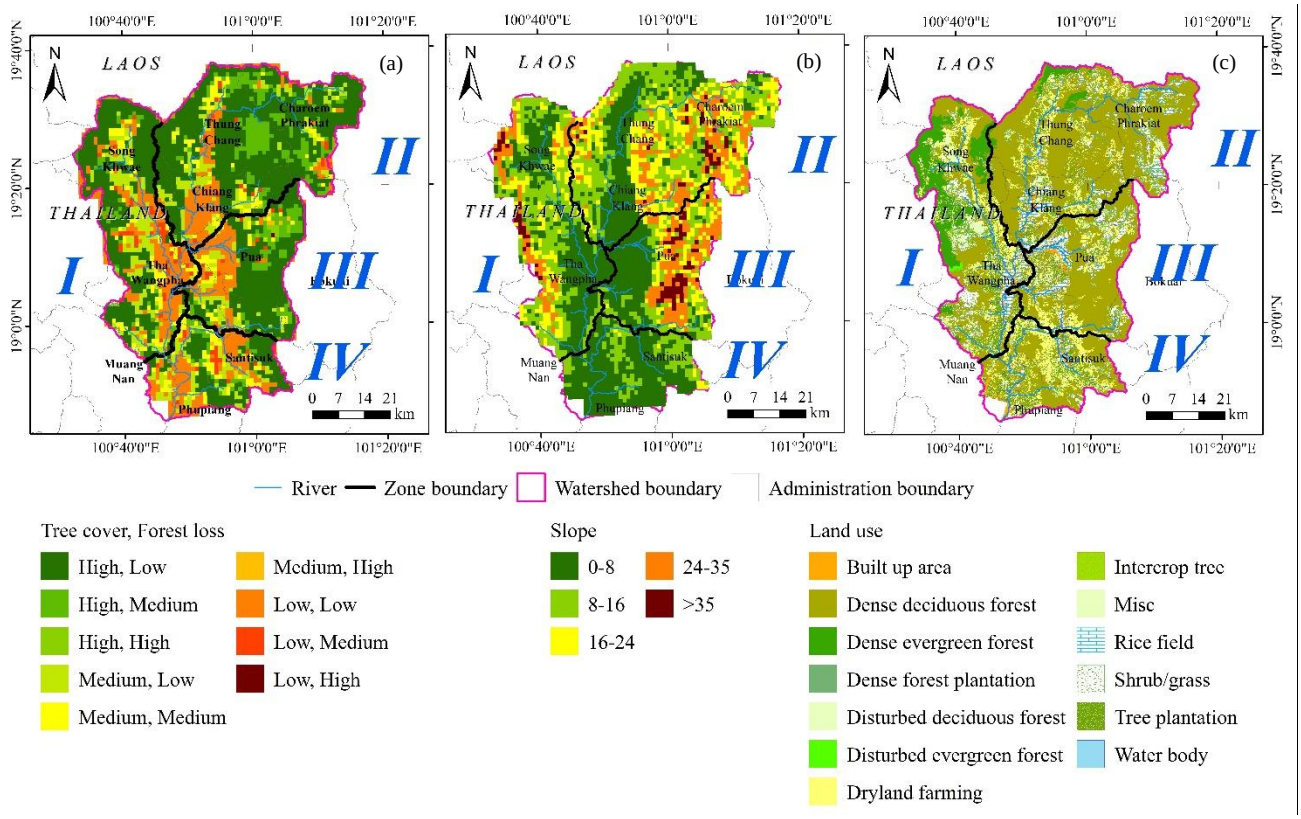


**Figure 9.** Ecological and anthropogenic factors: (a) tree cover and forest loss, (b) slope, and (c) land use

**Table 2.** Upper Nan Watershed morphometry

| Sub-W | MSO | DD | CR | ER | RR |
|---|---|---|---|---|---|
| 13 | 2 | 0.32 | 0.23 | 0.63 | 95.8 |
| 14 | 3 | 0.49 | 0.10 | 0.62 | 81.7 |
| 15* | 4 | 0.28 | 0.24 | 0.57 | 34.6 |
| 25* | 5 | 0.35 | 0.18 | 0.59 | 13.7 |

Note: MSO, maximum stream order; DD, drainage density; CR, circulatory ratio; ER, elongation ratio; RR, relief ratio; *, lowest.

## 3.2 Discussion

*3.2.1 Correlation between meteorological and hydrological drought*

Our analysis revealed a significant positive correlation between MD and HD in the UNW, with the strongest correlation observed during the wet season. This finding aligns with the results of previous studies, such as the works by Huang et al. (2017) and Xu et al. (2021) in China, which identified similar patterns between MD and agricultural drought.

The identified DPT in the UNW ranges from 2 to 11 months, with a predominant period of 2 to 5 months. This range aligns with those found in previous studies in Asian regions, highlighting similarities and nuanced differences. For instance, Li et al. (2022) reported DPTs in the Arid Region of Northeast Asia (ARNA) of 1-3 months in summer and autumn and 5-12 months in spring and winter. The shorter DPTs in summer and autumn align with the findings for the UNW during the wet season, while the longer DPTs in the ARNA reflect its extreme climatic conditions. Ding et al. (2021b) observed a DPT range of 1-12 months across their study area in China, reflecting diverse local conditions similar to those in the UNW. Luo et al. (2023), in the neighboring Lancang-Mekong River Basin, found DPTs of 2-11 months with a predominant period of 2-5 months; considering the similar climatic conditions, their result reinforces our findings for the UNW. While the similar lag times between the UNW and other watersheds can be attributed to common monsoon patterns, local factors such as the soil characteristics, land use, and watershed morphometry lead to differences in specific DPT values. Understanding these nuances is crucial for developing effective, region-specific drought management strategies.

The similar lag times between the UNW and other watersheds are due to common regional climatic patterns and monsoon-influenced hydrological processes. However, local factors such as soil characteristics, land use, and watershed morphometry cause differences in the specific DPT values. For instance, the ARNA's extreme climatic conditions result in greater seasonal DPT variations compared to the more stable UNW. Understanding these nuances is crucial for tailoring region-specific drought management strategies.

The transition from MD to HD is driven by several mechanisms:

Soil moisture depletion: During periods of reduced rainfall (MD), soil moisture decreases significantly, leading to reduced groundwater recharge (Cao et al., 2016; Khaki et al., 2018). This depletion of soil moisture affects surface water flow, contributing to the onset of HD.

Evapotranspiration: High temperatures associated with MD increase evapotranspiration rates, further depleting soil moisture and reducing surface water availability (Condon et al., 2020; Vahmani et al., 2021). This accelerated loss of water from the soil and water bodies intensifies HD conditions.

Runoff reduction: Reduced rainfall during MD leads to decreased runoff into rivers and streams (Bai et al., 2023; Nippgen et al., 2016). With less water entering the watershed's hydrological system, streamflow diminishes, exacerbating HD.

These mechanisms collectively explain the observed correlation between MD and HD and the identified DPTs in the UNW. Understanding these processes is crucial for effective drought management and mitigation strategies.

*3.2.2 Influence of global and local climatic factors*

This study highlights the significant impact of global teleconnection factors, such as ENSO, DMI, and PDO, on drought conditions in the UNW. Our XWT analysis showed a statistically significant negative correlation between these factors and both rainfall and evaporation. Ueangsawat and Jintrawet (2013) also noted ENSO's influence on short-term rainfall patterns in northern Thailand. However, the UNW's mountainous location may lessen the overall effect of these factors. Local climatic factors, particularly rainfall, have a more substantial impact on the DPT than air temperature. Higher-rainfall areas tend to have a decreased DPT, supporting Luo et al.'s (2023) findings that lower rainfall correlates with shorter DPTs. The lack of a consistent spatial pattern between the air temperature and DPT may be due to the coarse resolution of ERA5 satellite imagery, indicating a need for higher-resolution data to better understand these dynamics.

*3.2.3 Role of physical and ecological factors*

Physical characteristics such as the slope and watershed morphometry significantly influence the DPT. Zones with steep slopes and thin soils, such as Zone III, exhibit shorter DPTs (1-2 months) due to their rapid runoff and limited water retention. Conversely, zones with gentler slopes and better soil retention, such as Zone I, show longer DPTs, as water is retained for longer, delaying the transition from MD to HD. This aligns with results from Lin et al. (2023), who found that steep slopes accelerate drought propagation by facilitating rapid water movement and reducing infiltration. Factors such as the drainage density and watershed shape also play crucial roles, with more compact and better-draining watersheds experiencing faster drought propagation due to their efficient water conveyance.

Ecological factors, particularly forest cover, play a complex role in drought dynamics. High evapotranspiration rates in forests can lead to shorter DPTs, but forests also provide water regulation services that can extend DPTs. Studies by Ding et al. (2021c) and Tarigan et al. (2018) supported the assertion that forests enhance base flow and reduce runoff velocity, mitigating the impacts of drought. Forested areas tend to have longer DPTs due to their improved soil moisture retention and slower runoff, while regions with significant forest loss exhibit shorter DPTs due to their faster runoff and lower groundwater recharge. These findings indicate that areas with higher forest cover and lower forest loss, such as Zones I, II, and III, experience longer DPTs than areas with significant forest loss, such as Zone IV.

*3.2.4 Impact of anthropogenic activities*

Human activities such as dryland farming and deforestation exacerbate drought by reducing DPTs. In Zone IV, extensive dryland farming and significant forest loss have led to shorter DPTs, contrasting with studies highlighting forests' role in water retention. Zone III's agricultural practices further intensify drought conditions. Yang et al. (2023) found that reservoir regulation reduced the likelihood of meteorological droughts becoming hydrological by

16% and decreased the duration and severity of long-lasting hydrological droughts by 18% and 37%, respectively. Li et al. (2021) reported that human activities influence seasonal drought dynamics, especially in winter, alleviating hydrological drought severity. Shah et al. (2021) noted that intensive irrigation, reservoir storage, and groundwater pumping in India significantly impact agricultural and hydrological droughts. Wang et al. (2021) observed that high percentages of cropland shorten the DPT due to increased water consumption. In the Upper Nan Watershed, deforestation and dryland farming in Zone IV have led to shorter DPTs, in accordance with Wang et al.'s (2021) findings, while the extensive agricultural practices in Zone III align with Shah et al.'s (2021) observations. These studies highlight the significant impact of human activities on DPTs and underscore the importance of sustainable practices to mitigate drought in regions such as the Upper Nan Watershed.

*3.2.5 Practical implication and future research*

Understanding DPTs in the UNW is crucial for effective water management and climate adaptation. Maintaining forest cover and regulating land use are vital for mitigating drought impacts, while sustainable agriculture and forest conservation enhance resilience. The study provides valuable insights but has its limitations, including the coarse ERA5 satellite imagery resolution and a focus on general patterns that may overlook fine-scale climatic variations. The findings could be further refined by including soil properties, groundwater dynamics, and detailed land use data.

Additionally, the use of the soil and water assessment tool (SWAT), a semi-distributed hydrological model, imposes limitations on capturing the spatial heterogeneity of regional moisture at a fine scale. Since the SWAT operates on hydrological response units (HRUs) rather than individual grid cells, it does not fully account for moisture variability across different spatial regions. Future studies could consider using fully distributed models such as the Variable Infiltration Capacity (VIC) model, which provides a higher spatial resolution and better captures moisture dynamics. This could improve the accuracy of drought simulations and allow for a more detailed understanding of spatial variability in moisture and water retention across the watershed.

The maximum Pearson's correlation coefficient (MPCC) may not fully capture non-linear relationships between meteorological and hydrological droughts, and model calibration could affect the accuracy. Deeper analyses are required to examine specific land use changes and agricultural practices, and findings specific to the UNW may not be generalizable to other regions.

Policymakers should focus on forest conservation, sustainable land use, adaptive agriculture, and efficient water management strategies, while considering regional and seasonal DPT variability. An understanding of global teleconnection factors and local climatic conditions can inform climate adaptation strategies. Integrated watershed management, robust drought monitoring, community engagement, and policy coordination are essential for comprehensive drought management, enhancing water security, and building resilience in the UNW and similar regions.

## 4. CONCLUSION

This study provides insights into the transition from meteorological drought (MD) to hydrological drought (HD) in the Upper Nan Watershed (UNW), Thailand, using the SPEI, the SSI, cross-wavelet transform (XWT), and Pearson's correlation analyses. A positive correlation between MD and HD was found, with drought propagation times (DPTs) that ranged from 2 to 5 months and were shorter during the dry season. Zones with high tree cover and low forest loss exhibited longer DPTs, while areas with significant deforestation and dryland farming had shorter DPTs, highlighting the impact of land use on drought severity. These results underscore the need for reforestation, sustainable forest management, and water-efficient agricultural practices to enhance water retention and reduce drought severity. Land use regulations must be implemented to prevent deforestation and conserve critical watershed areas. Future research should use higher-resolution data, explore soil properties, and establish long-term monitoring programs. Policymakers should integrate these findings into their decision making, prioritize comprehensive drought management plans, and invest in data collection and analysis infrastructure to enhance drought resilience, mitigate socio-economic impacts, and promote sustainable development in the UNW and similar regions.

## ACKNOWLEDGEMENTS

We extend our gratitude to DAAD and the Southeast Asian Regional Center for Graduate Study

and Research in Agriculture (SEARCA) for funding this research.

## REFERENCES

Abbas S, Kousar S. Spatial analysis of drought severity and magnitude using the standardized precipitation index and streamflow drought index over the Upper Indus Basin, Pakistan. Environment Development Sustainability 2021;23(10):15314-40.

Bai X, Zhao W, Liu H, Zhang Y, Yang Q, Liu J, et al. Effects of precipitation changes and land-use alteration on streamflow: A comparative analysis from two adjacent catchments in the Qilian Mountains, arid northwestern China. Frontiers in Environmental Science 2023;11:Article No. 1097049.

Cao G, Scanlon BR, Han D, Zheng C. Impacts of thickening unsaturated zone on groundwater recharge in the North China Plain. Journal of Hydrology 2016;537:260-70.

Condon LE, Atchley AL, Maxwell RM. Evapotranspiration depletes groundwater under warming over the contiguous United States. Nature Communications 2020;11:Article No. 873.

Dalezios NR, Blanta A, Spyropoulos NV. Assessment of remotely sensed drought features in vulnerable agriculture. Natural Hazards and Earth System Science 2012;12(10):3139-50.

Ding Y, Gong X, Xing Z, Cai H, Zhou Z, Zhang D, et al. Attribution of meteorological, hydrological and agricultural drought propagation in different climatic regions of China. Agricultural Water Management 2021a;255:Article No. 106996.

Ding Y, Xu J, Wang X, Cai H, Zhou Z, Sun Y, et al. Propagation of meteorological to hydrological drought for different climate regions in China. Journal of Environmental Management 2021b;238:Article No. 111980.

Ding Y, Wang F, Mu Q, Sun Y, Cai H, Zhou Z, et al. Estimating land use/land cover change impacts on vegetation response to drought under 'Grain for Green' in the Loess Plateau. Land Degradation and Development 2021c;32(17):5083-98.

Fedele G, Locatelli B, Djoudi H, Colloff MJ. Reducing risks by transforming landscapes: Cross-scale effects of land-use changes on ecosystem services. PLoS One 2018;13(4): e0195895.

Gu L, Chen J, Yin J, Xu C-Y, Chen H. Drought hazard transferability from meteorological to hydrological propagation. Journal of Hydrology 2020;585:Article No. 124761.

Hansen MC, Potapov PV, Moore R, Hancher M, Turubanova SA, Tyukavina A, et al. High-resolution global maps of 21st-century forest cover change. Science 2013;342(6160):850-3.

Huang S, Li P, Huang Q, Leng G, Hou B, Ma L. The propagation from meteorological to hydrological drought and its potential influence factors. Journal of Hydrology 2017;547:184-95.

Kartika FD, Wijayanti P. Drought disaster modeling using drought index: A systematic literature review. IOP Conference Series: Earth and Environmental Science 2023;1190:Article No. 012026.

Khaki M, Forootan E, Kuhn M, Awange JL, van Dijk AIJM, Schumacher M, et al. Determining water storage depletion within Iran by assimilating GRACE data into the W3RA hydrological model. Advanced in Water Resources 2018;114:1-18.

Li C, Zhang X, Yin G, Xu Y, Hao F. Evaluation of drought propagation characteristics and influencing factors in an Arid Region of Northeast Asia (ARNA). Remote Sensing 2022;14(14):Article No. 3307.

Li Z, Huang S, Zhou S, Leng G, Liu D, Huang Q, et al. Clarifying the propagation dynamics from meteorological to hydrological drought induced by climate change and direct human activities. Journal of Hydrometeorology 2021;22(9):2359-78.

Lin Q, Wu Z, Zhang Y, Peng T, Chang W, Guo J. Propagation from meteorological to hydrological drought and its application to drought prediction in the Xijiang River Basin, South China. Journal of Hydrology 2023;617:Article No. 128889.

Luo X, Luo X, Ji X, Ming W, Wang L, Xiao X, et al. Meteorological and hydrological droughts in the Lancang-Mekong River Basin: Spatiotemporal patterns and propagation. Atmospheric Research 2023;293:Article No. 106913.

Nippgen F, McGlynn BL, Emanuel RE, Vose JM. Watershed memory at the Coweeta Hydrologic Laboratory: The effect of past precipitation and storage on hydrologic response. Water Resources Research 2016;52(3):1673-95.

Paiboonvorachat C, Oyana TJ. Land-cover changes and potential impacts on soil erosion in the Nan Watershed, Thailand. International Journal of Remote Sensing 2011;32(21):6587-609.

Plangoen P, Babel M. Projected rainfall erosivity changes under future climate in the Upper Nan Watershed, Thailand. Journal of Earth Science and Climatic Change 2014;5(10):Article No. 242.

Satriagasa MC, Tongdeenok P, Kaewjampa N. Assessing the implication of climate change to forecast future flood using SWAT and HEC-RAS model under CMIP5 climate projection in Upper Nan Watershed, Thailand. Sustainability 2023;15(6):Article No. 5276.

Shah D, Shah HL, Dave HM, Mishra V. Contrasting influence of human activities on agricultural and hydrological droughts in India. Science of the Total Environment 2021;774:Article No. 144959.

Tarigan S, Wiegand K, Sunarti, Slamet B. Minimum forest cover required for sustainable water flow regulation of a watershed: A case study in Jambi Province, Indonesia. Hydrology and Earth System Sciences 2018;22(1):581-94.

Ueangsawat K, Jintrawet A. The impacts of ENSO phases on the variation of rainfall and stream flow in the Upper Ping River Basin, Northern Thailand. Environment and Natural Resources Journal 2013;11(2):97-119.

Vahmani P, Jones AD, Li D. Will Anthropogenic warming increase evapotranspiration? examining irrigation water demand implications of climate change in California. Earth's Future 2021;10:e2021EF002221.

Vicente-Serrano SM, Beguería S, López-Moreno JI. A multiscalar drought index sensitive to global warming: The standardized precipitation evapotranspiration index. Journal of Climate 2010;23(7):1696-718.

Wan W, Zhao J, Li H, Mishra A, Hejazi M, Lu H, et al. A holistic view of water management impacts on future droughts: A global multimodel analysis. Journal of Geophysical Research Atmospheres 2018;123:5947-72.

Wang J, Wang W, Cheng H, Wang H, Zhu Y. Propagation from meteorological to hydrological drought and its influencing

factors in the Huaihe River Basin. Water 2021;13(14):Article No. 1985.

Xu Y, Zhang X, Hao Z, Singh VP, Hao F. Characterization of agricultural drought propagation over China based on bivariate probabilistic quantification. Journal of Hydrology 2021;598:Article No. 126194.

Xu Y, Zhang X, Wang X, Hao Z, Singh VP, Hao F. Propagation from meteorological drought to hydrological drought under the impact of human activities: A case study in Northern China. Journal of Hydrology 2019;579:Article No. 124147.

Yang H, Ma F, Yuan X. The role of human activities in the weakening of the propagation relationship between meteorological and hydrological droughts in the Heihe River Basin. Hydrological Process 2023;37(7):e14946.